AMERICAN SOCIETY FOR MICROBIOLOGY | Journal of Virology®

PATHOGENESIS AND IMMUNITY

What a Difference a Gene Makes: Identification of Virulence Factors of Cowpox Virus

Aistė Tamošiūnaitė,[a] Saskia Weber,[b] Timo Schippers,[a] Annika Franke,[b] Zhiyong Xu,[a] Maria Jenckel,[b] Florian Pfaff,[b] Donata Hoffmann,[b] Maegan Newell,[a] B. Karsten Tischer,[a] Martin Beer,[b] Nikolaus Osterrieder[a]

[a]Institut für Virologie, Freie Universität Berlin, Berlin, Germany

[b]Institute of Diagnostic Virology, Friedrich-Loeffler-Institut, Greifswald-insel Riems, Germany

Aistė Tamošiūnaitė, Saskia Weber, and Timo Schippers contributed equally to this article.

ABSTRACT Cowpox virus (CPXV) is a zoonotic orthopoxvirus (OPV) that causes spillover infections from its animal hosts to humans. In 2009, several human CPXV cases occurred through transmission from pet rats. An isolate from a diseased rat, RatPox09, exhibited significantly increased virulence in Wistar rats and caused high mortality compared to that caused by the mildly virulent laboratory strain Brighton Red (BR). The RatPox09 genome encodes four genes which are absent in the BR genome. We hypothesized that their gene products could be major factors influencing the high virulence of RatPox09. To address this hypothesis, we employed several BR-RatPox09 chimeric viruses. Using Red-mediated mutagenesis, we generated BR-based knock-in mutants with single or multiple insertions of the respective RatPox09 genes. High-throughput sequencing was used to verify the genomic integrity of all recombinant viruses, and transcriptomic analyses confirmed that the expression profiles of the genes that were adjacent to the modified ones were unaltered. While the *in vitro* growth kinetics were comparable to those of BR and RatPox09, we discovered that a knock-in BR mutant containing the four RatPox09-specific genes was as virulent as the RatPox09 isolate, causing death in over 75% of infected Wistar rats. Unexpectedly, the insertion of *gCPXV0030* (*g7tGP*) alone into the BR genome resulted in significantly higher clinical scores and lower survival rates matching the rate for rats infected with RatPox09. The insertion of *gCPXV0284*, encoding the BTB (broad-complex, tramtrack, and bric-à-brac) domain protein D7L, also increased the virulence of BR, while the other two open reading frames failed to rescue virulence independently. In summary, our results confirmed our hypothesis that a relatively small set of four genes can contribute significantly to CPXV virulence in the natural rat animal model.

IMPORTANCE With the cessation of vaccination against smallpox and its assumed cross-protectivity against other OPV infections, waning immunity could open up new niches for related poxviruses. Therefore, the identification of virulence mechanisms in CPXV is of general interest. Here, we aimed to identify virulence markers in an experimental rodent CPXV infection model using bacterial artificial chromosome (BAC)-based virus recombineering. We focused our work on the recent zoonotic CPXV isolate RatPox09, which is highly pathogenic in Wistar rats, unlike the avirulent BR reference strain. In several animal studies, we were able to identify a novel set of CPXV virulence genes. Two of the identified virulence genes, encoding a putative BTB/POZ protein (CPXVD7L) and a B22R-family protein (CPXV7tGP), respectively, have not yet been described to be involved in CPXV virulence. Our results also show that single genes can significantly affect virulence, thus facilitating adaptation to other hosts.

KEYWORDS cowpox virus, pathogenesis, virulence factors, zoonotic infections

Citation Tamošiūnaitė A, Weber S, Schippers T, Franke A, Xu Z, Jenckel M, Pfaff F, Hoffmann D, Newell M, Tischer BK, Beer M, Osterrieder N. 2020. What a difference a gene makes: identification of virulence factors of cowpox virus. J Virol 94:e01625-19. https://doi.org/10.1128/JVI.01625-19.

Editor Rozanne M. Sandri-Goldin, University of California, Irvine

Address correspondence to Martin Beer, martin.beer@fli.de, or Nikolaus Osterrieder, no.34@fu-berlin.de.

Received 27 September 2019
Accepted 27 September 2019
Accepted manuscript posted online 23 October 2019
Published 6 January 2020

Cowpox virus (CPXV) is a model orthopoxvirus (OPV) for several reasons. First, CPXV has the broadest host range of all known orthopoxviruses and is capable of productively infecting various species, including humans (1–4). Second, rising numbers of CPXV infections in humans and animals have been reported over the last few years and have resulted in CPXV being considered a (re)emerging virus with increasing epizootic and zoonotic potential (5–11). It is important to note that the name "cowpox" is a misnomer, since wild rodents, specifically, voles, represent the main reservoir host for the virus (12, 13). However, spillover infections from accidental hosts, including cats and pet rats, to humans occur frequently, mostly through skin lesions (14–19). The resulting human infections are generally self-limiting with typical pox lesions at the site of virus entry. However, the virus can also cause systemic and fatal disease in immunocompromised patients (20, 21). CPXV possesses the largest genome and the most complete genetic repertoire of all known OPVs (22–25), and the remarkable set of host range and immunomodulatory genes, in particular, might allow the virus to evolve and increase its virulence (21, 22).

It is becoming increasingly clear that CPXV is polyphyletic with several distinct clades (12, 26, 27). The frequent isolation of new strains and accessibility to whole-genome sequencing data (currently, more than 80 strains are deposited in GenBank) have increased the complexity of the CPXV phylogenetic tree and also demonstrate the close genetic relationship to human smallpox virus (13, 28, 29). However, despite the impressive number of field isolates sequenced, only rarely were CPXV strains compared with each other regarding their pathogenicity in experimental animal models. Interestingly, different CPXV strains resulted in quite variable mortality rates ranging from 0% to 100% in mice and rats, despite similar growth kinetics *in vitro*, and increased virulence did not correlate with stronger cytopathic effects (CPE) in cell culture (30, 31). It seems, therefore, that the variation of *in vivo* virulence is a direct effect of genetic differences among the strains, and it is tempting to speculate that the presence or absence of single virulence factors is responsible for different disease outcomes. However, such factors can be reliably identified only using *in vivo* studies, since even three-dimensional (3D) skin cultures that should represent a more natural model of infection failed to recapitulate the differences in virulence detected in the animal model (32).

CPXV Brighton Red (BR) is a commonly used laboratory strain that was originally isolated in 1937 from the finger of a cowman and maintained by serial passage, first in guinea pigs and rabbits and later in cell culture (33, 34). Despite the clear genomic adaptations to cell culture conditions that laboratory strains of many viruses usually undergo, CPXV BR is still considered a CPXV reference strain.

In 2009, a new strain was isolated from a diseased pet rat, which had bitten and infected two girls (13, 35). The isolate was named RatPox09 and exhibited *in vitro* viral growth characteristics similar to those of the reference strain, CPXV BR (31, 32). *In vivo* experiments using Wistar rats and pet rats demonstrated, however, that animals infected with RatPox09 developed severe and often fatal disease, whereas the infection of mice or rats with CPXV BR resulted in no or very mild clinical symptoms (31, 35, 36). RatPox09 is an ideal example of a CPXV strain which adapted after spillover infection to rats and causes severe clinical disease. The complete genomic sequence of RatPox09 was determined by high-throughput sequencing and compared with that of BR, which revealed a nucleotide sequence identity of 92% (31). Inspection of the sequences revealed four unique open reading frames (ORFs) which are present in the RatPox09 genome but absent in the BR genome (31). These genes were named *gCPXV0002*, *gCPXV0003*, *gCPXV0284*, and *gCPXV0030* after their relative position in the genome (31), but information on the encoded gene products is still scarce. *gCPXV0002* shares 99% nucleotide sequence identity with the CPXV gene encoding the *N*-methyl-D-aspartate (NMDA) receptor-like protein, and we refer to this gene as *gNMDAr* here. The function of the protein in CPXV infection is unknown (12), but the NMDAr protein sequence has 98% amino acid identity with vaccinia virus (VACV) Golgi apparatus antiapoptotic protein (vGAAP) (37). GAAPs are highly conserved and resident in the Golgi apparatus.

They inhibit apoptosis induced by intrinsic and extrinsic stimuli and, in addition, form cation-selective ion channels that regulate Ca^{2+} levels and fluxes that participate in cell adhesion and migration (37, 38). NMDAr has a high amino acid sequence identity with different lifeguard (Lfg) proteins in cattle (78% identity), mice (74% identity), and rats (74% identity). Members of the Lfg family are widely distributed in eukaryotes, and some of them have been reported to play a cytoprotective role during apoptosis (39). In the VACV infection model of mice, the loss of vGAAP was associated with increased virulence (37). *gCPXV0003* has 99% identity with the VACV gene encoding the cytokine response modifier E (CrmE), a known virulence factor of VACV (40). CrmE is a secreted molecule, belongs to the tumor necrosis factor (TNF) receptor superfamily, and blocks the binding of TNF to high-affinity TNF receptors on the cell surface (40). *gCPXV0284* shares 92% nucleotide sequence identity with the gene that encodes D7L, a broad-complex, tramtrack, and bric-à-brac (BTB) domain protein of CPXV strain GRI-90 (D7L). However, the function of the D7L protein is unknown (25). *gCPXV0030* has 99% nucleotide sequence identity with the gene encoding the CPXV 7-transmembrane G protein-coupled receptor-like protein (*7tGP*) (12). Despite its misleading name, multiple structure analysis tools predict only one transmembrane domain and two poxvirus B22R-like domains between amino acids (aa) 10 and 777 as well as aa 786 and 1053 (41). B22 proteins are conserved in representatives of most poxviruses, which may indicate a long evolutionary history and host adaptation. In fact, some poxviruses contain multiple copies of genes encoding these proteins (42). Monkeypox B22 proteins directly inhibit T cells by rendering them unresponsive to stimulation by the T cell receptor and major histocompatibility complex (MHC)-dependent antigen presentation or to MHC-independent stimulation (43). Deletion of the B22 homolog in ectromelia virus (ECTV) resulted in a significant reduction of virulence in the relevant mouse model (42). In addition, two ORFs, *gCPXV158* (*gATI*) and *gCPXV159* (*gp4c*), were markedly different in the RatPox09 and BR genomes (31). The amino acid sequence of RatPox09 p4c (A26) has a 59-aa truncation at the N terminus, which likely is responsible for its failure to direct intracellular mature virions (IMVs) in acidophilic-type inclusion bodies (ATI) (31), while the BR p4c gene is disrupted due to a premature stop codon introduced by a frameshift mutation (44). Furthermore, CPXV BR and RatPox09 ATI-encoding genes show modifications in length and sequence, particularly in the repeat regions, even though the translational initiation and stop codons of these two ORFs are identical. The overall nucleotide sequence identity of CPXV BR and RatPox09 ATI-encoding genes is 87%. Both ATI and p4c are vital for incorporation of IMVs into A-type inclusion bodies (44–46). It is assumed that ATIs are proteinaceous matrices which shield infectious particles after they are released into the environment (47). Moreover, genome comparison also revealed many single nucleotide polymorphisms (SNPs) that were scattered all over the genome of RatPox09 (31). The impact of these SNPs on the coding potential of the virus is currently unclear.

We hypothesized that the additional full-length gene products of RatPox09 rather than individual SNPs would significantly contribute to the increased virulence observed in previous infection studies using Wistar rats (31, 35), in which the virulence would simulate the real-world situation previously observed in pet rats in the field (48).

In order to test our hypothesis, we inserted individual RatPox09 genes as well as combinations thereof into the CPXV BR genome by Red mutagenesis of BR cloned into a bacterial artificial chromosome (BAC). To address the impact of the minor sequence polymorphisms that are spread all over the genome, we also generated BR-RatPox09 chimeric viruses with large genomic segments exchanged between the two strains. This allowed us to screen for potential additional virulence factors in an unbiased fashion. To exclude the possibility of any secondary-site mutations introduced during the mutagenesis, the genomic integrity of all viruses was verified by whole-genome sequencing and comprehensive transcriptomic analyses. Finally, animal experiments conducted in infected rats allowed the analysis of the generated hybrid viruses and comparison with the parental BR and RatPox09 viruses.

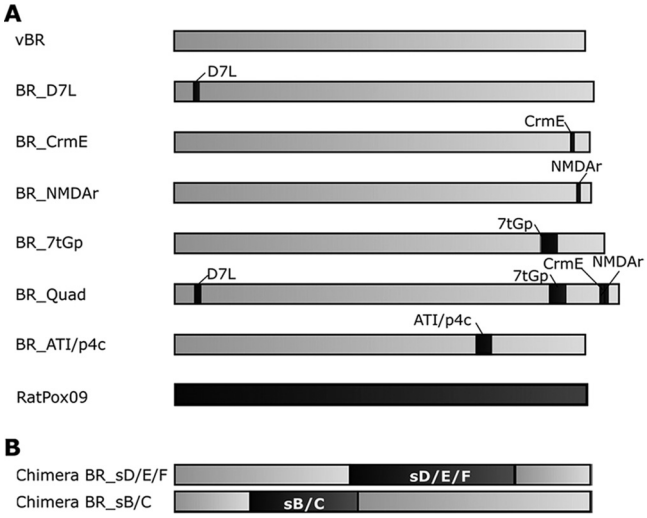

FIG 1 Schematic illustration of newly generated BAC knock-in mutants (A) and the generated chimeric viruses (B). Gray boxes, BR sequences; black boxes, RatPox09 sequences.

RESULTS

Generation of CPXV BR knock-in mutants. First, we generated BR-based mutant viruses that harbored the unique RatPox09 ORFs (*gD7L*, *gCrmE*, *gNMDAr*, *g7tGP*) either individually or as multiple gene knock-ins at their original loci (Fig. 1A). Mutant viruses were constructed using the full-length pBRF BAC clone. Moreover, a CPXV BR mutant virus harboring both RatPox09 *gATI* and *gp4c* was generated. After Red recombination, all final BACs were verified by restriction fragment length polymorphism (RFLP) analysis and Sanger sequencing of the modified genomic loci (data not shown). Virus mutants were reconstituted on Vero cells from the modified BAC clones, and the genomic integrity of the viruses was verified by whole-genome sequencing (data are available by request). Apart from the desired modifications, no secondary mutations or rearrangements were present in the genomes of the final mutant viruses (data not shown). Furthermore, transcriptomic analysis confirmed all of the mRNA transcripts of the inserted sequences and unchanged transcription levels of the respective adjacent genes (Fig. 2).

Generation of CPXV BR-RatPox09 chimeric viruses. In order to identify additional virulence genes in RatPox09, we swapped large genomic segments of the low-virulence strain BR with the corresponding regions of RatPox09. For this purpose, we divided the RatPox09 genome into seven segments of 20 to 40 kb in size and named the fragments A to G. To allow homologous recombination, the sequence of each segment was chosen such that it contained at least 800 bp of overlapping, identical sequences between the two strains. In order to generate the chimeras, we first deleted the respective genome regions in pBRF by Red mutagenesis. This step was necessary to avoid homologous recombination events during reinsertion of the segments. We confirmed successful deletion from pBRF of the segments in question by RFLP analysis and sequencing (data not shown). In a second step, we amplified the RatPox09-derived regions of interest by high-fidelity PCR and again used Red recombineering to reinsert segments at the deletion sites of pBRF. Using this strategy, we generated chimeric viruses containing segments B and C or segments D, E, and F in combination (chimeras BR_sB/C and BR_sD/E/F, respectively) (Fig. 1B).

***In vitro* characterization of the mutants and chimeras does not reveal growth differences.** All CPXV chimeras or CPXV knock-in mutants were compared to the respective reference strains, BR and RatPox09, by single and multistep growth kinetics in cell culture. In four independent experiments using technical duplicates as internal controls, growth kinetics were determined in Vero 76 cells using a multiplicity of infection (MOI) of 0.01 or an MOI of 3.

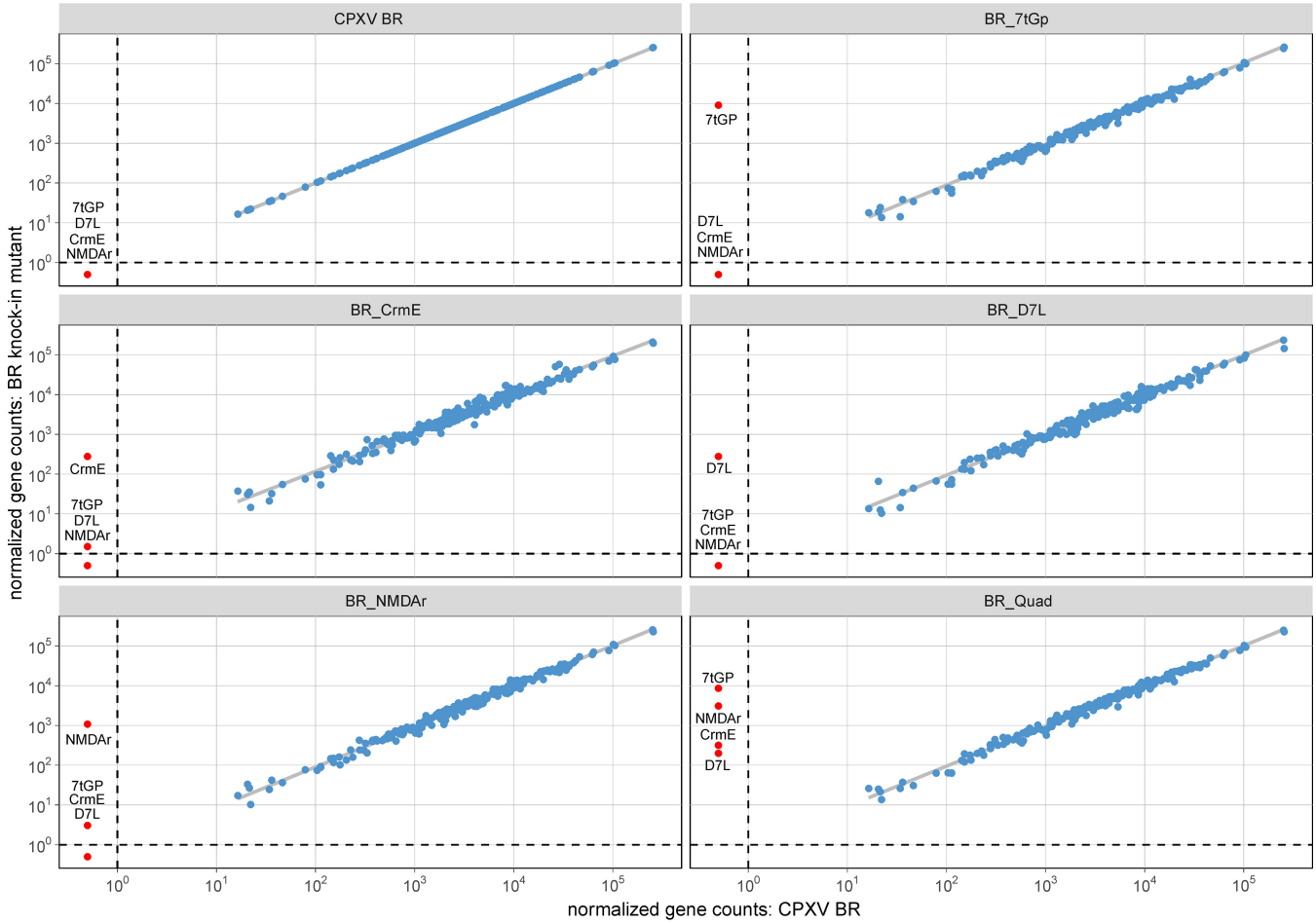

FIG 2 Transcriptomic analysis. The normalized gene count for CPXV BR is compared to the normalized gene count for the knock-in mutant CPXVs.

BR and RatPox09 exhibited similar viral titers with no significant differences ($P > 0.05$ in all cases). The differences in the viral titers detected from any of the tested knock-in mutants or chimeric viruses did not exceed 1 order of magnitude (data not shown). At 24 h postinfection (hpi), titers of $\sim 10^5$ 50% tissue culture infective doses ($TCID_{50}$) ml^{-1} (MOI, 0.01) or $\sim 10^6$ (MOI, 3) were determined, regardless of whether the cells were infected with BR, RatPox09, or any of the mutants or chimeras. There were also no significant differences between the titers at 48 hpi, regardless of whether an MOI of 0.01 or an MOI of 3 was used (data not shown).

***In vivo* characterization of mutants and chimeras.** In order to explore any gain of function of the different mutants and chimeras *in vivo*, we inoculated Wistar rats and used the experimentally well-defined virus isolates BR, BAC-derived BR (vBR), and RatPox09 as controls.

Clinical signs: high clinical scores for rats infected with BR_7tGP and BR_D7L/CrmE/NMDAr/7tGP. After intranasal infection, the first clinical signs were respiratory in nature and included a prominent nasal discharge at 3 to 7 days postinfection (dpi), regardless of the virus used for infection. The higher clinical scores presented in Fig. 3 over this time span are attributed to respiratory symptoms. In addition, pox-like lesions on the skin and mucous surfaces were observed, typically at later time points during the infection (>8 dpi). As expected, the BR strain caused no or only mild symptoms of nasal discharge, decreased activity, and rough fur but no skin lesions, resulting in clinical scores ranging from 1 to 2 throughout the animal experiment (Fig. 3A and B). As seen in earlier studies (35, 49), RatPox09 caused severe symptoms that included inflated stomachs, moderate to severe respiratory distress, loss of body weight, and pox

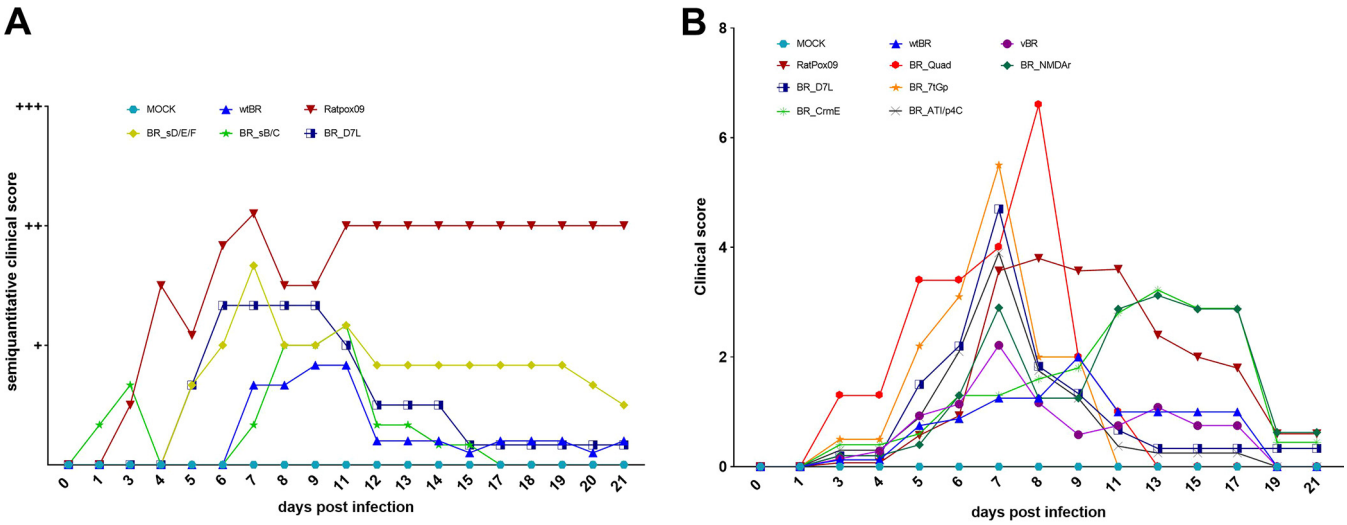

FIG 3 Rat CPXV infection clinical score over time. Rats infected with $10^{5.5}$ $TCID_{50}$ per animal were clinically evaluated semiquantitatively on a daily basis in experimental setup 1 (A), while in experimental setup 2, evaluation by a quantitative clinical score system was used (B).

lesions on the skin (>8 dpi). Clinical scores (Table 1) reached a peak of approximately 4 at 8 dpi (Fig. 3B).

In particular, infections with the BR_7tGP virus and the BR_D7L/CrmE/NMDAr/7tGP virus (referred to as the BR_Quad virus from here on) resulted in clinical scores at earlier time points even higher than those achieved by infection with reference strain RatPox09 (Fig. 3B). This observation was also correlated to increased mortality (see "Mortality: BR_7tGP and BR_Quad are highly virulent and lethal" below). Nevertheless, animals that recovered from infection with BR_Quad or BR_7tGP did not exhibit skin lesions.

The scores induced by the BR knock-in mutants BR_ATI/p4C and BR_D7L exhibited a peak at about 7 dpi, which clustered with those induced by RatPox09, while the scores induced by BR_NMDAr were almost similar to those induced by RatPox09 at later time points (11 dpi to 17 dpi). Reflecting the delayed onset of respiratory symptoms, only a minority of animals developed skin lesions.

All tested recombinant viruses caused severe symptoms, as evidenced by the accumulation of high clinical scores (Fig. 3B). However, the clinical scores induced by chimeric viruses in the Wistar rat model did not exceed the clinical scores induced by RatPox09 infection (Fig. 3A). In order to analyze the kinetics of the clinical signs induced by the recombinant knock-in viruses, we calculated the start, the time point of the peak, and the duration of the observed clinical signs as well as the peak scores and the scores at the beginning and the end of the symptomatic period (Tables 2 and 3). While the duration of clinical signs was not significantly different between the groups, the maximum values of the clinical scores induced by the different viruses exhibited significant differences when comparisons between BR and RatPox09 and between BR and BR_Quad were made (Table 4).

Mortality: BR_7tGP and BR_Quad are highly virulent and lethal. Two mutant viruses led to a dramatic reduction in the survival of infected Wistar rats, namely, BR_7tGP and BR_Quad, where survival rates of only 20% to 35% were recorded. These rates were comparable to those observed after RatPox09 infection. Interestingly, the mortality in the BR_Quad-infected group was the highest, and only 20% of the inoculated animals survived. However, the differences in survival rates between the groups inoculated with the mutant and RatPox09 were not significant ($P \geq 0.05$). Nevertheless, RatPox09 and BR_Quad resulted in survival rates significantly lower than those achieved with the vBR control ($P \leq 0.05$) in all instances (Table 4). All other chimeras and mutant viruses caused mortalities that matched the mortality after

TABLE 1 Clinical scores used to evaluate CPXV-infected rats

Clinical parameter	No. of points
Body temp	
Above 36°C	0
35–36°C	1
34–35°C	2
Below 34°C	3
Activity	
Normal	0
Moderate	1
Inactive	2
Nasal discharge	
Absent	0
Doubtful	1
Clearly present	2
Body wt loss	
Absent	0
>10%	1
>20%	2
Respiratory distress	
Normal breathing	0
Light	1
Moderate	2
Severe	3
Wheezing	
Absent	0
Present	1
Pox lesions	
Absent	0
Present	1
Inflated stomach	
Absent	0
Present	1
Rough fur	
Absent	0
Present	1

infection with BR (approximately 72 to 100% survival) (Fig. 4). Since the Wistar rats used in the different experiments were outbred and therefore not genetically identical, a certain level of variation of survival rates between the experiments was to be expected and also recorded. The survival rates of animals infected with BR varied from 75% in the first experimental setup to 100% in the second one. Similarly, rats infected with RatPox09 had a survival rate of 29% in experimental setup 1 and 36% in the second setup. Most importantly, however, virus mutants that caused low survival rates similar to or even lower than those caused by RatPox09, namely, BR_7tGP and BR_Quad (also containing the gene for 7tGP), always produced clinical scores that matched the highest clinical scores evaluated (Fig. 3B).

Finally, one mock-infected animal was euthanized due to malocclusion of the dentition. The virus genome was not detectable in either buccal swab or organ tissue samples in that case (Fig. 4A).

Virus shedding: no enhanced shedding of recombinant CPXV. Oropharyngeal shedding was detected in all groups (Fig. 5). Generally, the first excretion of virus was recorded at between 3 and 5 dpi, and most rats showed positive buccal swab samples between 5 and 7 dpi (Tables 2 and 3). Generally, animals infected with RatPox09 shed more virus than the animals in all other groups ($10^{3.1}$ $TCID_{50}$/ml at 7 dpi). Interestingly,

TABLE 2 Median parameters describing CPXV shedding and kinetics of swab specimens from the different groups

Parameter	Units	Value for swabs from rats infected with[a]:							
		vBR ($n = 13$)	RatPox09 ($n = 14$)	BR_Quad ($n = 8$)	BR_NMDAr ($n = 7$)	BR_D7L ($n = 10$)	BR_7tGP ($n = 10$)	BR_CrmE ($n = 10$)	BR_ATI/p4c ($n = 9$)
T_{max}	Days	7 (5, 9)	7 (7, 9.5)	7 (5, 7)	6 (5, 9)	5 (5, 7.5)	5 (5, 5)	9 (6.5, 9)	7 (5, 9)
T_{start}	dpi	5 (5, 5)	5 (5, 7)	5 (4.5, 7)	5 (5, 5)	5 (5, 5)	4 (3, 5)	5 (3, 7)	5 (3.5, 5)
T_{end}	dpi	7 (5, 11)	8 (7, 11)	7 (7, 7)	9 (7, 10.5)	7 (7, 11)	5 (5, 7)	11 (10.5, 11)	7 (7, 9)
Duration	Days	3 (1, 5)	3 (3, 5)	1 (1, 3.5)	5 (3, 7)	3 (3, 7)	2.5 (1:3)	5 (4.75, 7)	4 (3, 5)
V_{max}	Log_{10} $TCID_{50}$/ml	2.313 (1.781, 3.031)	3.75 (2.875, 3.906)	1.813 (1.625, 2.125)	2.125 (1.906, 3.5)	2.5 (2.094, 2.938)	1.625 (1.625, 1.875)	2.625 (2.219, 3.156)	2.25 (2, 2.75)
V_{start}	Log_{10} $TCID_{50}$/ml	1.75 (1.75, 2.25)	2.188 (1.875, 3.25)	1.625 (1.625, 1.823)	1.875 (1.656, 2)	2.25 (1.875, 2.5)	1.625 (1.625, 1.875)	2 (1.875, 2.156)	1.875 (1.625, 2.094)
V_{end}	Log_{10} $TCID_{50}$/ml	2.25 (1.75, 2.594)	3.5 (2.719, 3.875)	1.75 (1.625, 2.031)	1.813 (1.75, 1.969)	1.75 (1.75, 1.906)	1.625 (1.625, 1.875)	1.875 (1.625, 2.313)	2 (1.781, 2.406)

[a]The data represent the median (the interval between the first and the third quartiles) calculated from the individual parameters. *n*, number of swabs.

TABLE 3 Median parameters describing CPXV kinetics of clinical scoring values for animals in the different groups

Parameter	Units	Value for rats infected with[a]:							
		vBR (n = 14)	RatPox09 (n = 14)	BR_Quad (n = 10)	BR_NMDAr (n = 10)	BR_D7L (n = 9)	BR_7tGP (n = 10)	BR_CrmE (n = 10)	BR_ATI/p4c (n = 10)
T_{max}	Days	7 (6.25, 11)	8 (7, 9)	8 (8, 8)	11 (7, 11)	7 (7, 7)	7 (7, 7)	13 (11, 13)	7.5 (7, 8)
T_{start}	dpi	5 (4.25, 6.75)	6 (5, 7)	3 (3, 5)	6 (5.25, 7)	5 (5, 5)	4 (3, 5)	5.5 (3, 6)	5.5 (3.5, 6)
T_{end}	dpi	17 (8, 17)	8.5 (7.25, 11)	8 (8, 8)	19 (17, 21)	8 (7, 11)	7 (7, 9)	17 (17, 20)	8 (7, 10.5)
CS_{max}	CS	2 (1.25, 2)	4.5 (4, 7)	7.5 (7, 8)	4 (3.25, 4.75)	3 (3, 9)	5.5 (3, 8)	3.5 (2, 4.75)	3 (2.25, 3)
CS_{start}	CS	1 (1, 1)	2 (1, 3)	2.5 (2, 4.5)	1 (1, 1)	2 (1, 2)	1.5 (1, 2)	1 (1, 1)	2 (1, 2)
CS_{end}	CS	1 (1, 2)	4.5 (3.25, 7)	7.5 (7, 8)	1 (1, 1)	2 (1, 9)	5.5 (2, 8)	2 (2, 2)	2.5 (1, 3)
S_{max}	Days	21 (21, 21)	8.5 (7.25, 21)	8 (8, 8)	21 (21, 21)	21 (7, 21)	7 (7, 21)	21 (21, 21)	21 (21, 21)
S_{end}	CS	0 (0, 0)	4.5 (1, 7)	7.5 (7, 8)	1 (0.25, 1)	1 (0, 9)	5.5 (0, 8)	0 (0, 1)	0 (0, 0)

[a]The data represent the median (the interval between the first and the third quartiles) calculated from the individual parameters. *n*, number of rats.

TABLE 4 Statistical evaluation of median parameters for the vBR-inoculated group in comparison to those for single- and multiple-knock-in mutants

Parameter	Unit of measurement	*P* value for vBR vs[a]:						
		RatPox09	BR_Quad	BR_NMDAr	BR_D7L	BR_7tGP	BR_CrmE	BR_ATI/p4c
T_{max}	d	0.1031	>0.9999	>0.9999	>0.9999	0.0161	0.501	>0.9999
T_{start}	dpi	0.1258	>0.9999	>0.9999	>0.9999	0.0498	>0.9999	>0.9999
T_{end}	dpi	0.0905	>0.9999	0.7744	0.4634	0.0297	0.0019	>0.9999
Duration of shedding	dpi	>0.9999	0.9723	0.2018	0.1243	0.7422	0.0186	>0.9999
V_{max}	log_{10} $TCID_{50}$/ml	<0.0001	0.0291	>0.9999	>0.9999	0.0061	>0.9999	>0.9999
V_{start}	log_{10} $TCID_{50}$/ml	<0.0001	>0.9999	>0.9999	0.4794	>0.9999	>0.9999	>0.9999
V_{end}	log_{10} $TCID_{50}$/ml	<0.0001	0.1663	0.1857	0.8106	0.0159	>0.9999	>0.9999
T_{max}	d	>0.9999	>0.9999	0.8033	>0.9999	>0.9999	<0.0001	>0.9999
T_{start}	dpi	>0.9999	0.0434	>0.9999	>0.9999	0.0915	0.8233	>0.9999
T_{end}	dpi	>0.9999	0.0878	0.2042	>0.9999	0.035	0.0878	0.5555
CS_{max}	CS	0.0257	0.0015	0.5054	0.0489	0.0445	>0.9999	>0.9999
CS_{start}	CS	0.0285	<0.0001	>0.9999	0.8623	0.6542	>0.9999	0.6542
CS_{end}	CS	0.1765	0.0052	>0.9999	0.4073	0.151	>0.9999	>0.9999
S_{max}	d	0.0348	0.0072	>0.9999	0.705	0.0783	>0.9999	>0.9999
S_{end}	CS	0.1236	0.0056	>0.9999	0.272	0.2038	>0.9999	>0.9999

$P < 0.05$	$P < 0.01$	$P < 0.001$	$P < 0.0001$

[a]Each cell contains the *P* value. The *P* values are color coded in the key at the bottom.

albeit the mutant viruses BR_7tGP and BR_Quad induced excessive mortality rates of up to 80% (Fig. 4), viral shedding was within the range of that achieved with BR, with virus titers being between $10^{0.74}$ and $10^{1.5}$ $TCID_{50}$/ml (at 5 to 7 dpi) (Fig. 5). This was confirmed by the statistical evaluation of shedding kinetics (Table 5): comparison of viral excretion titers (determined as the time of peak shedding [T_{max}], the time at the start of the shedding period [T_{start}], and the time at the end of virus shedding [T_{end}]) of RatPox09 with those of BR, BR_Quad, and BR-7tGP displayed highly significant differences.

Viral load in organ samples. The distribution of viral DNA in various organs was determined by quantitative PCR. All rats that succumbed to CPXV infection scored positive for virus DNA in turbinate samples, regardless of which virus mutant or chimera was used for inoculation. Turbinate samples taken from Wistar rats euthanized at 5 dpi were positive as well. Other organs scored positive only when animals succumbed or were examined at 5 dpi (data not shown).

Serology. Blood serum samples from all rats that succumbed to infection or animals dissected on day 5 postinfection (p.i.) were negative for antibodies, while antibodies against the mutants or chimeras were detectable in all serum samples obtained on 21 or 28 dpi (data not shown).

DISCUSSION

With the eradication and subsequent cessation of vaccination against smallpox, zoonotic OPV infections are on the rise due to waning immunity in the human population, and an increasing number of humans are becoming susceptible to poxvirus infections every year. Such infections include those caused by monkeypox virus (MPXV) in Central/West Africa, CPXV in Europe, and VACV in Brazil and India (50–54). Molecular characterization of OPVs isolated from different geographic locations or hosts is therefore of high importance for understanding their geographic distribution, variability, and evolution, as well as for monitoring the emergence of atypical OPV strains with enhanced virulence.

It has been documented that CPXV strains vary significantly regarding their virulence in rodent models, with mortality rates ranging from 0 to 100% (31, 35, 36, 49). Our studies and those of other laboratories have shown that these *in vivo* differences

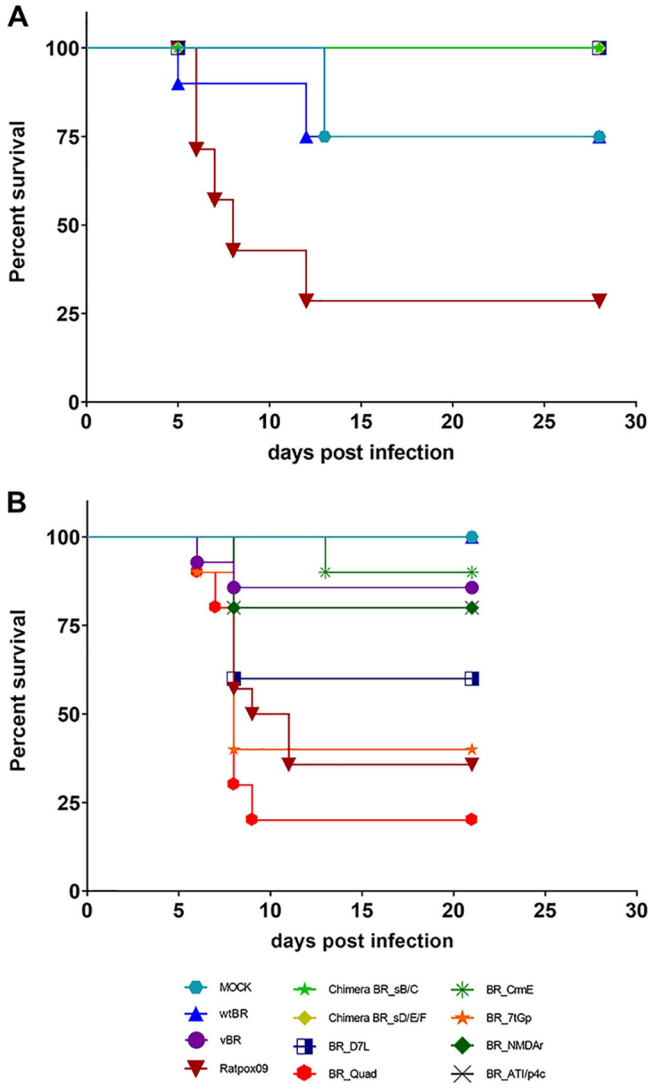

FIG 4 Rat survival over time in two experiments. Rats were infected with $10^{5.5}$ $TCID_{50}$ per animal of wtBR, RatPox09, chimeric viruses, and the D7L knock-in virus (A), and in the final two experiments, rats were infected with $10^{5.5}$ $TCID_{50}$ per animal of wtBR, vBR, RatPox09, BR_ sF, and the knock-in mutants (B).

cannot be recapitulated by *in vitro* assays that focus exclusively on cytopathic effects in cell culture. Similarly, a three-dimensional (3D) skin model as a possible replacement for animal experiments for the identification of CPXV virulence factors failed to address the virulence of individual mutants: The histopathological and immunohistochemical studies showed that the 3D model reflected the development of pox lesions in normal skin very well, but it did not allow the differentiation between virulent and avirulent CPXV strains (32). Two lessons could be learned from that study. First, *in vivo* experiments still present the gold standard for the identification of CPXV genes that control virulence. Second, and more importantly, virulence factors appear to have important functions that impact the viral replication cycle only in complex and diverse multicellular organisms. These functions include diversions of host defense mechanisms, particularly evasion of the immune system, and, hence, can currently be identified only *in vivo*. In addition, the role in countering host defenses exerted by certain proteins should be studied in relevant animal host models to avoid incompatibilities, as was demonstrated for CPXV studies in laboratory mice and subsequent studies using ECTV in the mouse footpad model (42, 55). Therefore, a matching pair of virus and host species should be evaluated. This goes hand in hand with the claim of biological congruence between the

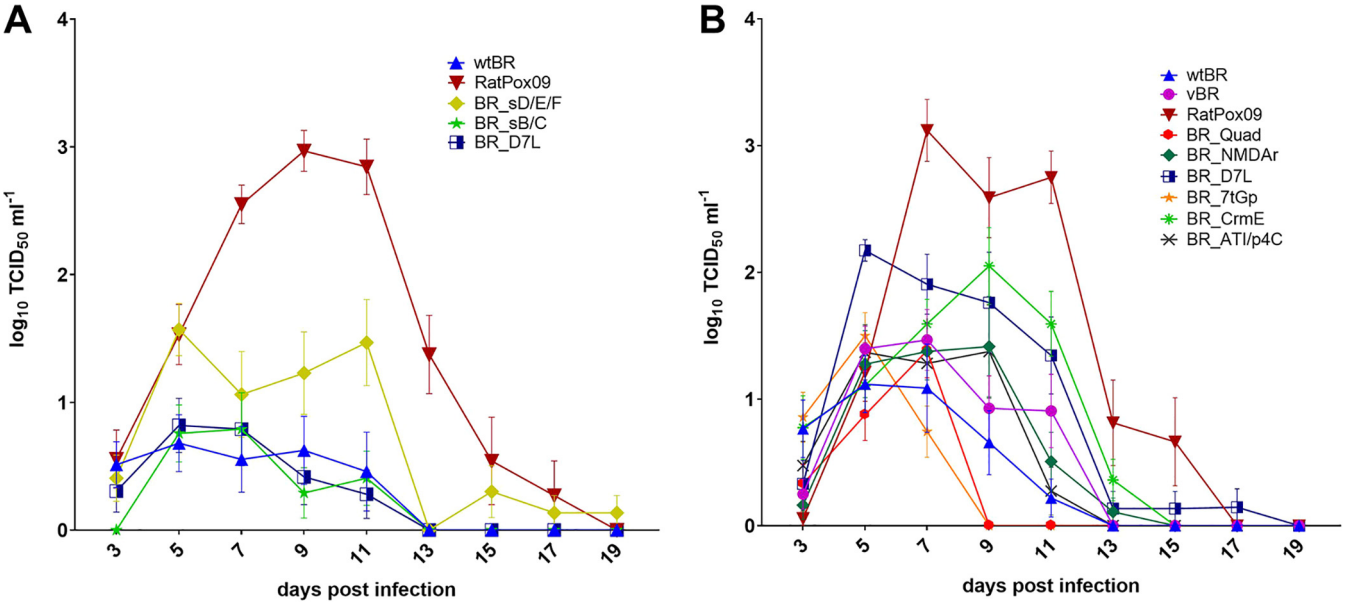

FIG 5 Viral shedding patterns of infected Wistar rats. In the initial two experiments, rats were infected with $10^{5.5}$ $TCID_{50}$ per animal of wtBR, RatPox09, chimeric viruses, and the D7L knock-in virus (A), and in the two follow-up experiments, rats were infected with $10^{5.5}$ $TCID_{50}$ per animal of wtBR, vBR, RatPox09, and the knock-in mutants (B).

properties of the test population and those of the target population as a central part of the construct validity proposed for the explanatory value of experimental findings (56). We contend that the use of the established CPXV-Wistar rat model provides a unique possibility to study pathogen determinants in a spillover animal model which closely mimics the situation in the field. However, this is connected to further challenges, like the variation of the noninbred animals themselves, but this, again, is likely a scenario that is much closer to that in the real world and reflects the field situation better than any inbred, and thus somewhat artificial, mouse model.

TABLE 5 Statistical evaluation of median parameters for the RatPox09-inoculated group in comparison to those for the single- and multiple-knock-in mutants

Parameter	Unit of measurement	*P* value for RatPox09 vs[a]:						
		vBR	BR_Quad	BR_NMDAr	BR_D7L	BR_7tGP	BR_CrmE	BR_ATI/p4c
T_{max}	d	0.1031	0.0368	0.3159	0.0154	<0.0001	>0.9999	0.1742
T_{start}	dpi	0.1258	0.4713	0.0205	0.0135	<0.0001	0.0306	0.0368
T_{end}	dpi	0.0749	0.0035	0.9975	0.9976	<0.0001	0.5913	0.221
Duration of shedding	dpi	>0.9999	0.0815	>0.9999	>0.9999	0.044	0.3426	>0.9999
V_{max}	log_{10} $TCID_{50}$/ml	<0.0001	<0.0001	<0.0001	<0.0001	<0.0001	<0.0001	<0.0001
V_{start}	log_{10} $TCID_{50}$/ml	<0.0001	<0.0001	0.0061	0.0575	<0.0001	0.0055	<0.0001
V_{end}	log_{10} $TCID_{50}$/ml	<0.0001	<0.0001	<0.0001	<0.0001	<0.0001	<0.0001	<0.0001
T_{max}	d	>0.9999	>0.9999	>0.9999	0.3947	0.3543	0.0012	0.5911
T_{start}	dpi	>0.9999	0.0434	>0.9999	>0.9999	0.0915	0.8233	>0.9999
T_{end}	dpi	0.7766	0.5537	0.0094	>0.9999	0.3333	0.0033	0.977
CS_{max}	CS	0.0257	>0.9999	>0.9999	>0.9999	>0.9999	0.35	>0.9999
CS_{start}	CS	0.0285	0.0096	0.2829	>0.9999	>0.9999	0.073	>0.9999
CS_{end}	CS	0.1339	0.5945	0.3806	0.9999	0.9996	0.1473	0.789
S_{max}	d	0.0348	>0.9999	0.163	>0.9999	>0.9999	0.0222	0.163
S_{end}	CS	0.1236	>0.9999	>0.9999	>0.9999	>0.9999	0.1144	0.6792

$P < 0.05$	$P < 0.01$	$P < 0.001$	$P < 0.0001$

[a]Each cell contains the *P* value. The *P* values are color coded in the key at the bottom.

In the study presented here, we show that recombineering of avirulent CPXV BR represents a workable platform to identify novel virulence genes of CPXV field isolates in the Wistar rat model. We employed two different approaches in our study. (i) *En passant* Red recombination was used to introduce six specific RatPox09 genes of interest into the BR genome. (ii) Furthermore, since whole-genome sequencing revealed small genetic mutations of unknown impact scattered all over the RatPox09 genome, we used an unbiased approach to generate BR-RatPox09 chimeric viruses in which combinations of multiple genome segments from RatPox09 replaced the authentic BR sequences. The introduced mutations were verified by whole-genome sequencing and further by complete transcriptomic analysis of the different recombinant viruses to ensure that the knock-in genes and neighboring genes were correctly transcribed. In each of the animal experiments, groups of rats infected with wild-type BR (wtBR), vBR, and RatPox09 served as controls and defined the virulence threshold ranging from low to high.

From our *in vivo* data, we can conclude that the gene encoding the protein 7tGP is responsible for a significant increase in the virulence of an avirulent CPXV laboratory strain. Reintroduction of the gene into the BR genome resulted in virulence levels that matched those of the highly virulent field isolate RatPox09. Moreover, the so-called quadruple mutant BR_Quad (BR_D7L/CrmE/NMDAr/7tGP), whose genome also encodes the 7tGP gene, caused significantly lower survival rates in infected rats than vBR or wtBR ($P \leq 0.05$, analysis of variance [ANOVA]). The protein encoded by the *g7tGP* gene has some similarity to poxviral proteins of the B21R/B22R family (41). Previous reports have suggested that the B21/B22R proteins of MPXV and CPXV render human T cells unresponsive to stimulation both by MHC-dependent antigen presentation and by MHC-independent stimulation (43, 55). However, the detailed functions of the B21/B22R protein MPXV197 and its CPXV homologue (CPXV219) have not yet been elucidated (43, 55). It is tempting to hypothesize that CPXV 7tGP might have an immunomodulatory function similar to that which is pivotal for the significantly increased virulence of BR_7tGP, and we are currently further investigating this hypothesis.

Nevertheless, the notion that a single gene in RatPox09 might be sufficient to transform a CPXV strain from a low-virulence to a high-virulence phenotype was unexpected. However, viral shedding, detected by the collection of buccal swab samples from animals infected with BR_7tGP, did not reach the levels seen in rats infected with RatPox09. The induction of clinical disease and lethal infection is therefore linked to CPXV 7tGP, while shedding in oral secretions is probably not. This leads to one speculative explanation: the mortality caused by 7tGP-positive orthopoxviruses could be related to less functional T cells in infected animals. In addition, the quadruple mutant BR_Quad also was not excreted as RatPox09 was, and thus, the insertion of *gD7L*, *gCrmE*, *gNMDAr*, and *g7tGP* increased the virulence significantly but not the excretion levels. The *in vivo*-detected viral replicative fitness of BR_7tGP and BR_Quad was clearly similar to that of RatPox09 (e.g., as measured by the organ viral load in the diseased rats).

Therefore, CPXV 7tGP is most likely a relevant virulence factor in our *in vivo* model. It is responsible for the observed highly virulent phenotype of CPXV in Wistar rats, consisting of (i) a prominent viral replication fitness in the animal, while (ii) excretion is impaired in this model. This is contrary to the findings for other animal viruses, where *in vivo* increases in virulence often lead to prominent viral shedding (57). The increased virulence and shedding are therefore related to the effects of multiple genes and, possibly, epistatic interactions between these genes.

The individual insertion of the two remaining unique RatPox09 genes, *gCrmE* and *gNMDAr*, resulted in only a nonstatistically significant increased virulence of BR. However, the rate of mortality in rats infected with BR_CrmE or BR_NMDAr was higher than that in rats infected with BR. The respective clinical scores were in the intermediate range, with an obvious and peculiar shift of the peak scores at late time points of the animal experiments. Homologues of both proteins in VACV have been the focus of

studies in the past: VACV CrmE is a soluble tumor necrosis factor alpha (TNF-α) receptor with both soluble and membrane viral tumor necrosis factor alpha receptor (vTNFR) activity and was shown to bind to rat, mouse, and human TNF-α and to protect against human, but not mouse or rat, TNF-mediated cytolysis *in vitro* (40, 58, 59). As expected, CPXV BR with RatPox09 CrmE inserted induced stronger symptoms than wtBR, a finding that is in full agreement with previous publications describing the effects of VACV infection. Deletion of *gCrmE* in the VACV strain USSR in an intranasal mouse infection model resulted in marked attenuation of the virus, whereas overexpression of the protein led to increased virulence (59). Nevertheless, all recorded symptoms were of a more general nature: severe clinical signs, such as pox skin lesions, were not detected in animals infected with wild-type or mutant viruses. Furthermore, the NMDAr homolog in VACV, viral GAAP (vGAAP; 98% similarity with RatPox09 NMDAr), and a human orthologue, human GAAP (hGAAP), were shown to protect cells from apoptosis derived from both intrinsic and extrinsic pathways (37).

The single insertion of the RatPox09 gene for D7L increased the virulence of BR to higher levels in one animal experiment, whereas BR_D7L did not cause mortality in the second experimental setup. As mentioned previously, we believe that the outbred status of animals could explain these differences. Depending on the function of the protein under investigation, the different genetic background could potentially influence the impact of certain virulence genes but not others. By the use of independently repeated experiments, this drawback was minimized. Generally, the use of outbred animals is admissible in the context of dominant factors to be evaluated. Nevertheless, we are currently exploring the function of D7L in CPXV virulence. The protein contains a predicted, N-terminally located BTB (broad-complex, tramtrack, and bric-à-brac)/POZ (for poxvirus and zinc finger) domain between amino acids 31 and 131 (41). BTB domain-encoding genes are found among eukaryotic and poxvirus genomes (60), and the domain itself functions as a docking station for protein-protein interactions (61). Unlike many poxviral BTB proteins, the BTB-only protein D7L misses a C-terminally located kelch domain, a protein interaction domain that mediates the proteasomal degradation of cellular substrates by ubiquitin ligase complexes. Mammalian BTB proteins were found to have diverse functions, from playing a part in embryogenesis to fulfilling important roles in the development of specialized lymphocyte effector cells. In many cases, they function as transcriptional suppressors (62–67).

Interestingly, none of the tested BR-RatPox09 chimeric viruses exhibited any significant increase in virulence above the BR baseline virulence, as measured by mortality (Fig. 4). We swapped the sequences of the genes for ATI and p4c in BR for the RatPox09 ATI and p4c gene sequences. However, BR_ATI/p4c failed to reach virulence levels comparable to those of RatPox09 (Fig. 3B and 4B).

In conclusion, proteins with putative immunomodulatory functions are potent virulence genes in many different viruses, including CPXV. Here, we identified CPXV *7tGP* especially to be a novel relevant factor modifying virulence in the well-established Wistar rat model. Interestingly, virulence was not linked to the levels of virus excretion. Our study also underlines the value of BAC mutagenesis when comparing highly adapted standard lab strains like BR—in the case of CPXV—to rodent-borne isolates. The targeted engineering of mutant viruses is easy and fast and, most importantly, has a low error rate, as confirmed by whole-genome sequencing. The seamless introduction of almost any desired modification, e.g., whole genes or even large fragments, allows the straightforward screening and identification of relevant virulence markers and fitness-related genes by *in vivo* animal model studies. Future studies will surely benefit from this versatile platform.

MATERIALS AND METHODS

Cell lines and viruses. African green monkey cells (Vero 76 cells; Collection of Cell Lines in Veterinary Medicine, Friedrich-Loeffler-Institut, Greifswald-Insel Riems, Germany) were grown and maintained in Eagle's minimal essential medium (MEM; Biochrom, Berlin, Germany) supplemented with 10% fetal calf serum (FCS; Biochrom) and kept at 37°C under a 5% CO_2 atmosphere. Chicken embryo cells (CECs) were prepared fresh from 10-day-old specific-pathogen-free (SPF) White Leghorn chicken embryos (Valo;

BioMedia GmbH, Osterholz-Scharmbeck, Germany) by a standard protocol (68). Cells were cultured in MEM containing 10% FCS and 100 U/ml penicillin (Fisher Scientific, Schwerte, Germany), 100 U/ml streptomycin (AppliChem GmbH, Darmstadt, Germany) and kept at 37°C under a 5% CO_2 atmosphere. CPXV strain Brighton Red (strain AF482758, kindly provided by Philippa Beard, University of Edinburgh, Edinburgh, UK), was cloned as a bacterial artificial chromosome (BAC) and termed pBRF (69). The CPXV rat isolate (RatPox09) was obtained in 2009 from a diseased pet rat in southern Germany. All CPXVs used in this study were propagated and titrated on Vero 76 cells or CECs. Fowlpox virus (FWPV; Nobilis-PD strain, kindly provided by D. Lüschow, Freie Universität Berlin, Berlin, Germany) was grown on CECs and used as the helper virus for the reconstitution of CPXVs. Virus stocks were prepared as described by Xu et al. (70).

Plasmid, mutant, and chimeric virus construction. The sequences of RatPox09 genes *gCPXV0002* (*gNMDAr*), *gCPXV0003* (*gCrmE*), *gCPXV0284* (*gD7L*), and *gCPXV0030* (*g7tGP*) and the combination of *CPXV158* (*gATI*) and *CPXV159* (*gp4c*), including the predicted promoter sequences, were amplified from CPXV RatPox09 viral DNA using PrimeSTAR GXL polymerase (TaKaRa, Clontech Laboratories, Inc., USA). The *g7tGP* sequence was cloned into the SacI and PstI unique restriction sites of the pUC19 plasmid (New England Biolabs, Frankfurt am Main, Germany). A kanamycin resistance cassette and an adjoining I-SceI site were amplified by PCR and inserted into unique restriction sites of the corresponding plasmid. The *gD7L*, *gCrmE*, and *gNMDAr* sequences were cloned into the BamHI and KpnI sites of the pEP-kanS2 high-copy-number plasmid containing an *aphAI*-I-SceI cassette (71, 72). In the case of *gATI-gp4c*, an SbfI restriction site upstream and a HindIII site downstream of the gene were used. Duplicate sequences for removal of the *aphAI* cassette were added to the transfer construct through 5-prime extensions of the primers. The transfer constructs were then used to insert the sequences of interest into the desired target sequences present in pBRF using a two-step Red recombination as described earlier (71, 72).

Red recombination was also used for the generation of chimeric viruses. For deletion of the segments of interest from pBRF and recovery of the segments of interest from RatPox09, PCR primers were designed to amplify the *aphAI* cassette from recombinant plasmid pEP-kanS2. Besides the marker cassette, the PCR fragments contained at each end 40 bp of sequences that were homologous to the target locus in the CPXV sequence. LongAmp *Taq* DNA polymerase (New England Biolabs) was used for this purpose. Plasmid and BAC DNAs were extracted by alkaline lysis and verified by restriction fragment length polymorphism (RFLP) analysis. PCR products overlapping the modified loci were confirmed by agarose gel electrophoresis, purified using a GF-1 AmbiClean nucleic acid extraction kit (Vivantis Technologies, Subang Jaya, Malaysia), and sequenced to verify the correct modification of the genome.

Reconstitution of infectious virus from BAC DNA. For virus reconstitution, Vero cells seeded in 6-well plates (1×10^6 cells per well) were transfected with 2 μg of purified plasmid or BAC DNA and 4 μl the FuGENE HD transfection reagent (Promega, Mannheim, Germany) according to the manufacturer's instructions. Chimeric viruses were generated by cotransfection of 1 μg of pBRF deletion mutant DNA diluted in 2 μl TE (Tris-EDTA) buffer together with 1 μg of RatPox09 segment-of-interest DNA diluted in 2 μl TE buffer. Transfected cultures were infected with 500 PFU of FWPV at 2 h after transfection. Since the BAC DNA used for virus reconstitution encodes the green fluorescent protein (GFP) under a late 4b FWPV promoter (69), virus reconstitution was monitored by examining GFP expression using an Axiovert S100 fluorescence microscope (Carl Zeiss, Jena, Germany). Newly reconstituted virus was than passaged not less than four times, in order to remove the helper virus. Later, mini-F vector sequences present in pBRF were removed and the thymidine kinase (TK) gene was repaired by transfection with a TK-containing plasmid.

High-throughput sequencing of full-length CPXV genomes. Full-genome sequencing of CPXV isolates was conducted as previously described (31). In brief, DNA was extracted from infected cell cultures using a High Pure PCR template preparation kit (Roche, Mannheim, Germany), and 0.5 to 1 μg of DNA was fragmented to approximately 300 bp using a Covaris M220 ultrasonicator (Covaris, Brighton, UK). Illumina-compatible sequencing libraries were prepared using NEXTflex DNA barcodes (Bioo Scientific, Austin, TX, USA) and SPRI works Fragment Library Cartridge II (Beckman Coulter, Fullerton, CA, USA) on a SPRI-TE library system (Beckman Coulter). Size exclusion of the library was done manually using AMPure XP magnetic beads (Beckman Coulter) and was controlled on a Bioanalyzer 2100 instrument (Agilent Technologies, Böblingen, Germany) using a high-sensitivity DNA chip and corresponding reagents. A Kapa library quantification kit (Kapa Biosystems, Wilmington, DE, USA) was further used for quantification of the final libraries. Sequencing was performed on an Illumina MiSeq sequencer using the MiSeq reagent kit, versions 2 and 3 (Illumina, San Diego, CA, USA).

***De novo* assembly and genome annotation of full-length CPXV genomes.** Raw reads were quality trimmed and assembled *de novo* using 454 sequencing system software (version 2.8; Roche, Mannheim, Germany), and the resulting contigs were arranged in order to match the CPXV genome. Draft CPXV genomes were further confirmed by reference-guided mapping (454 sequencing system software) using the –rst 0 parameter with respect to their repetitive genomic termini. The mean genomic coverage of each full-length CPXV sequence exceeded the minimal acceptable coverage of 20. Full-length CPXV sequences were annotated analogously to the nomenclature of the CPXV BR reference strain (strain AF482758) as described elsewhere (31).

Transcript expression analyses of CPXV knock-in mutants. Total RNA was extracted from Vero cells infected with CPXV BR or CPXV knock-in mutants using the TRIzol reagent (Life Technologies, Carlsbad, CA, USA) in combination with an Agencourt RNAdvance tissue kit (Beckman Coulter, Krefeld, Germany) on a KingFisher 96 Flex magnetic particle processor (Thermo Fisher Scientific Inc., Schwerte, Germany). During extraction, DNA was digested on-bead using an RNase-free DNase set (Qiagen, Hilden, Germany). Subsequently, the polyadenylated RNA fraction was extracted from a mixture of 5 μg total

TABLE 6 Design of animal experiments[a]

Expt	Group	No. of animals/group	Virus strain	Duration of experiment (dpi)	Tissues sampled at autopsy
1	Inoculated	8	Chimera BR_sB/C, chimera BR_sD/E/F, or BR_D7L	28[b]	Turbinates, trachea, lung, liver, spleen, skin, bladder
	Control	4	wtBR or RatPox09	28[b]	Turbinates, trachea, lung, liver, spleen, skin, bladder
2A	Inoculated	10	BR_CrmE or BR_NMDAr	21	Turbinates, trachea, lung, liver, spleen, skin
	Control	8	wtBR, vBR, or RatPox09	21	Turbinates, trachea, lung, liver, spleen, skin
2B	Inoculated	10	BR_D7L, BR_7tGP, BR_ATI/p4c, or BR_ Quad	21	Turbinates, trachea, lung, liver, spleen, skin
	Control	6	vBR or RatPox09	21	Turbinates, trachea, lung, liver, spleen, skin

[a]All animals were inoculated with the virus at a dose of $10^{5.5}$ 50% tissue culture infective doses ($TCID_{50}$) intranasally when they were 6 weeks of age, and buccal swab specimens were collected every 2 days. dpi, days postinoculation.
[b]Two animals from both the inoculated and the control groups were euthanized and autopsied at 5 dpi.

RNA and a supplemented internal control (ERCC ExFold RNA spike-in mix 1; Invitrogen, Carlsbad, CA, USA) using a Dynabeads mRNA Direct microkit (Invitrogen). The quantity and quality of the RNA were observed at each step using a NanoDrop 1000 spectrophotometer (Peqlab, Erlangen, Germany) and an Agilent 2100 bioanalyzer (Agilent Technologies, Böblingen, Germany). Strand-specific Ion Torrent-compatible libraries were constructed using an Ion Total RNA-Seq kit (version 2; Life Technologies) following the manufacturer's instructions. After quantification using a Kapa Ion Torrent library quantification kit (Kapa Biosystems, Wilmington, MA, USA), the libraries were sequenced on an Ion Torrent S5XL system (Life Technologies) using appropriate sequencing reagents.

For data analysis, raw reads were quality trimmed, and the remaining adapters were cut using 454 sequencing system software (version 3.0; Roche; Mannheim, Germany). Trimmed reads were then mapped against 233 coding DNA sequences (CDSs) from CPXV BR and the CDSs of RatPox09 genes *gCPXV0002* (*gNMDAr*), *gCPXV0003* (*gCrmE*), *gCPXV0284* (*gD7L*), and *gCPXV0030* (*g7tGP*) using the Bowtie2 program (version 2.3.5.1) (73). The matching reads were then quantified and transformed using Salmon software (version 0.14.1) (74) running in strand-specific alignment-based mode with 100 bootstrap replicates. The transformed read counts for each gene were then compared between the CPXV BR reference strain and the CPXV knock-in mutants using R (version 3.6.0) (75) and R studio (version 1.2.1335) software.

***In vitro* characterization: replication kinetics.** Vero cells from overnight cultures were infected with CPXV chimeras or CPXV knock-in mutants at a multiplicity of infection (MOI) of either 0.01 or 3. CPXV RatPox09, wtBR and BAC-derived BR (vBR) were used as references. After infection, cells were incubated for 60 min at 37°C. Afterwards, the cells were washed three times with phosphate-buffered saline (PBS), and then fresh culture medium was added. Samples were obtained at 6 different time points (0 h, 6 h, 12 h, 24 h, 48 h, and 72 h) as biological duplicates. Virus titers from the different time points were determined by an endpoint dilution assay with two technical replicates. The virus titers were calculated as the number of $TCID_{50}$ per milliliter using the Spearman-Kärber algorithm (76, 77).

***In vivo* characterization of chimeras and mutants.** The animal protocols were evaluated by the responsible ethics committee of the State Office for Agriculture, Food Safety and Fishery in Mecklenburg-Western Pomerania, Germany, and approval was obtained (approval number LALFF M-V 7221.3-1-020/13).

The animal numbers and the design of all experiments are summarized in Table 6. Initially, we inoculated 8 mixed-sex Wistar rats (outbred; Charles River, Sulzfeld, Germany) at 6 weeks of age with the double chimera BR_sB/C, the triple chimera BR_sD/E/F, or the BR_D7L knock-in mutant virus (experimental setup 1). The dose of the inoculum was $10^{5.5}$ $TCID_{50}$ per animal and was applied intranasally. CPXV RatPox09 and wtBR were used as controls. Over a period of 21 days, the animals were clinically evaluated on a daily basis and buccal swab specimens (Bakteriette; EM-TE Vertrieb, Hamburg, Germany) were taken every second day. At day 5 postinfection (p.i.), 2 rats per group were humanely killed. Individual organ tissue samples (turbinates, trachea, lung, liver, spleen, skin) were taken. Serum was sampled from the surviving animals at day 28 p.i., when the animals were humanely killed for autopsy and individual organ tissue samples were collected: rhinarium, trachea, lung, liver, spleen, kidney, skin, and bladder.

The experimental design of the animal studies performed here exactly followed that published previously for infection experiments with CPXV BR and RatPox09 in Wistar rats (31, 35, 49). This initial animal experiment had a duration of 28 days (experimental setup 1); since there was no change in the development of disease seen at 20 dpi, the following two animal experiments were conducted for only 21 days (experimental setup 2).

In the second experimental setup, we infected 10 Wistar rats (per virus) either with the single-gene-knock-in mutants (BR_D7L, BR_CrmE, BR_NMDAr, BR_7tGP) or with the multiple-gene-knock-in mutants (BR_ATI/p4c, BR_D7L/CrmE/NMDAr/7tGP). In addition to CPXV RatPox09, wtBR and BAC-derived BR were included as controls. Moreover, we developed a quantitative clinical score point system, which allowed for an objective evaluation of the clinical status of the individual infected animals (Table 1) and analysis of the kinetics of the symptomatic period (Tables 2 and 3). Animals that reached the experimental endpoint were euthanized. Buccal swab specimens were taken every other day, and the rats were

humanly euthanized at day 21 p.i. for autopsy and sampling (rhinarium, trachea, lung, liver, spleen, kidney, skin, serum). The clinical score point system was used only for experimental setup 2.

Determination of viral loads from buccal swab and organ tissue samples. Buccal swab samples were resuspended in 2 ml cell culture medium containing antibiotics (enrofloxacin, 1% [Bayer, Leverkusen, Germany]; amphotericin-gentamicin, 0.2% [Thermo Fisher Scientific Inc., Schwerte, Germany]; lincomycin, 0.5% [WDT, Garbsen, Germany]). The organ samples were transferred into 1 ml cell culture medium supplemented with 10% fetal calf serum (FCS) and antibiotics (1% penicillin-streptomycin; Biochrom GmbH, Berlin, Germany). The reaction tubes also contained stainless steel beads (diameter, 5 mm), which allowed mechanical homogenization (TissueLyser II; Qiagen, Hilden, Germany). Viral DNA was extracted from all buccal swab and organ tissue samples by using a BioSprint 96 instrument and a NucleoMag Vet kit (Macherey-Nagel, Berlin, Germany). OPV-specific DNA was detected by quantitative PCR (31). In addition, the viral loads of the samples were determined by an endpoint dilution assay and are given as the number $TCID_{50}$ per milliliter, calculated using the Spearman-Kärber algorithm (76, 77). The serum samples were analyzed by an indirect immunofluorescence test (31).

Bioinformatics and statistical analysis. Analysis of homologous poxvirus sequences, as well as the prediction of protein domains and functions, was performed using the NCBI BLAST, PFAM (Protein Families Database; http://pfam.xfam.org), and VectorNTI (version 9.1; Invitrogen, Darmstadt, Germany) software packages and was based on the OPV sequences available at the NIAID Virus Pathogen Database and Analysis Resource (ViPR) (78) through the website http://www.viprbrc.org/ and GenBank (79). GraphPad Prism software (GraphPad Software, La Jolla, CA, USA) was used for statistical evaluation. To describe the viral shedding kinetics in the Wistar rat model, we used median parameters in temporal units to determine the time of the start of the shedding period (T_{start}), the time of peak shedding (T_{max}), and the time of the end of virus shedding (T_{end}) (80). We also ascertained the initial virus titer shed (V_{start}), the peak viral titer shed (V_{max}), and the final virus titer shed (V_{end}) and characterized the viral shedding period as that time when viral titers of >1.625 $\log_{10}$ $TCID_{50}$ ml^{-1} were detected. For clinical scoring, we determined T_{start}, T_{max}, and T_{end} (in temporal units), as well as the clinical score (CS) units at the start of the shedding period (CS_{start}), at the time of peak shedding (CS_{max}), and at the end of virus shedding (CS_{end}). The data were truncated to keep virus-positive samples as well as CS-positive animals. Survival data were screened for the number of days that animals survived an infection (S_{max}) and the clinical scores when the animals left the experiments (S_{end}). We tested the association of individual parameters between the groups and animals infected with vBR or RatPox09.

One-way ANOVA with the Bonferroni correction ($P < 0.05$) was performed to determine whether the results were significantly different between the groups.

ACKNOWLEDGMENTS

We thank Doris Junghans and Mareen Lange for their excellent technical assistance.

This project was funded by German Research Foundation SPP1596 project BE5187, awarded to M.B. and N.O.

REFERENCES

1. Chantrey J, Meyer H, Baxby D, Begon M, Bown KJ, Hazel SM, Jones T, Montgomery WI, Bennett M. 1999. Cowpox: reservoir hosts and geographic range. Epidemiol Infect 122:455–460. https://doi.org/10.1017/s0950268899002423.
2. Coras B, Essbauer S, Pfeffer M, Meyer H, Schroder J, Stolz W, Landthaler M, Vogt T. 2005. Cowpox and a cat. Lancet 365:446. https://doi.org/10.1016/S0140-6736(05)17836-2.
3. Hemmer CJ, Littmann M, Lobermann M, Meyer H, Petschaelis A, Reisinger EC. 2010. Human cowpox virus infection acquired from a circus elephant in Germany. Int J Infect Dis 14(Suppl 3):e338–e340. https://doi.org/10.1016/j.ijid.2010.03.005.
4. Martina BE, van Doornum G, Dorrestein GM, Niesters HG, Stittelaar KJ, Wolters MA, van Bolhuis HG, Osterhaus AD. 2006. Cowpox virus transmission from rats to monkeys, the Netherlands. Emerg Infect Dis 12:1005–1007. https://doi.org/10.3201/eid1206.051513.
5. Becker C, Kurth A, Hessler F, Kramp H, Gokel M, Hoffmann R, Kuczka A, Nitsche A. 2009. Cowpox virus infection in pet rat owners: not always immediately recognized. Dtsch Arztebl Int 106:329–334. https://doi.org/10.3238/arztebl.2009.0329.
6. Campe H, Zimmermann P, Glos K, Bayer M, Bergemann H, Dreweck C, Graf P, Weber BK, Meyer H, Buttner M, Busch U, Sing A. 2009. Cowpox virus transmission from pet rats to humans, Germany. Emerg Infect Dis 15:777–780. https://doi.org/10.3201/eid1505.090159.
7. Kinnunen PM, Holopainen JM, Hemmila H, Piiparinen H, Sironen T, Kivela T, Virtanen J, Niemimaa J, Nikkari S, Jarvinen A, Vapalahti O. 2015. Severe ocular cowpox in a human, Finland. Emerg Infect Dis 21:2261–2263. https://doi.org/10.3201/eid2112.150621.
8. Kurth A, Straube M, Kuczka A, Dunsche AJ, Meyer H, Nitsche A. 2009. Cowpox virus outbreak in banded mongooses (*Mungos mungo*) and jaguarundis (*Herpailurus yagouaroundi*) with a time-delayed infection to humans. PLoS One 4:e6883. https://doi.org/10.1371/journal.pone.0006883.
9. Matz-Rensing K, Ellerbrok H, Ehlers B, Pauli G, Floto A, Alex M, Czerny CP, Kaup FJ. 2006. Fatal poxvirus outbreak in a colony of New World monkeys. Vet Pathol 43:212–218. https://doi.org/10.1354/vp.43-2-212.
10. Ninove L, Domart Y, Vervel C, Voinot C, Salez N, Raoult D, Meyer H, Capek I, Zandotti C, Charrel RN. 2009. Cowpox virus transmission from pet rats to humans, France. Emerg Infect Dis 15:781–784. https://doi.org/10.3201/eid1505.090235.
11. Świtaj K, Kajfasz P, Kurth A, Nitsche A. 2015. Cowpox after a cat scratch—case report from Poland. Ann Agric Environ Med 22:456–458. https://doi.org/10.5604/12321966.1167713.
12. Carroll DS, Emerson GL, Li Y, Sammons S, Olson V, Frace M, Nakazawa Y, Czerny CP, Tryland M, Kolodziejek J, Nowotny N, Olsen-Rasmussen M, Khristova M, Govil D, Karem K, Damon IK, Meyer H. 2011. Chasing Jenner's vaccine: revisiting cowpox virus classification. PLoS One 6:e23086. https://doi.org/10.1371/journal.pone.0023086.
13. Mauldin MR, Antwerpen M, Emerson GL, Li Y, Zoeller G, Carroll DS, Meyer H. 2017. Cowpox virus: what's in a name? Viruses 9:E101. https://doi.org/10.3390/v9050101.
14. Carletti F, Bordi L, Castilletti C, Di Caro A, Falasca L, Gioia C, Ippolito G, Zaniratti S, Beltrame A, Viale P, Capobianchi MR. 2009. Cat-to-human orthopoxvirus transmission, northeastern Italy. Emerg Infect Dis 15:499–500. https://doi.org/10.3201/eid1503.080813.
15. Elsendoorn A, Agius G, Le Moal G, Aajaji F, Favier AL, Wierzbicka-Hainault E, Beraud G, Flusin O, Crance JM, Roblot F. 2011. Severe ear chondritis due to cowpox virus transmitted by a pet rat. J Infect 63:391–393. https://doi.org/10.1016/j.jinf.2011.06.004.
16. Hobi S, Mueller RS, Hill M, Nitsche A, Loscher T, Guggemos W, Stander S,

Rjosk-Dendorfer D, Wollenberg A. 2015. Neurogenic inflammation and colliquative lymphadenitis with persistent orthopox virus DNA detection in a human case of cowpox virus infection transmitted by a domestic cat. Br J Dermatol 173:535–539. https://doi.org/10.1111/bjd.13700.
17. Kurth A, Wibbelt G, Gerber HP, Petschaelis A, Pauli G, Nitsche A. 2008. Rat-to-elephant-to-human transmission of cowpox virus. Emerg Infect Dis 14:670–671. https://doi.org/10.3201/eid1404.070817.
18. Vogel S, Sardy M, Glos K, Korting HC, Ruzicka T, Wollenberg A. 2012. The Munich outbreak of cutaneous cowpox infection: transmission by infected pet rats. Acta Derm Venereol 92:126–131. https://doi.org/10.2340/00015555-1227.
19. Vorou RM, Papavassiliou VG, Pierroutsakos IN. 2008. Cowpox virus infection: an emerging health threat. Curr Opin Infect Dis 21:153–156. https://doi.org/10.1097/QCO.0b013e3282f44c74.
20. Eis-Hubinger AM, Gerritzen A, Schneweis KE, Pfeiff B, Pullmann H, Mayr A, Czerny CP. 1990. Fatal cowpox-like virus infection transmitted by cat. Lancet 336:880. https://doi.org/10.1016/0140-6736(90)92387-w.
21. Essbauer S, Pfeffer M, Meyer H. 2010. Zoonotic poxviruses. Vet Microbiol 140:229–236. https://doi.org/10.1016/j.vetmic.2009.08.026.
22. Esposito JJ, Knight JC. 1985. Orthopoxvirus DNA: a comparison of restriction profiles and maps. Virology 143:230–251. https://doi.org/10.1016/0042-6822(85)90111-4.
23. Gubser C, Hue S, Kellam P, Smith GL. 2004. Poxvirus genomes: a phylogenetic analysis. J Gen Virol 85:105–117. https://doi.org/10.1099/vir.0.19565-0.
24. Meyer H, Totmenin A, Gavrilova E, Shchelkunov S. 2005. Variola and camelpox virus-specific sequences are part of a single large open reading frame identified in two German cowpox virus strains. Virus Res 108:39–43. https://doi.org/10.1016/j.virusres.2004.07.011.
25. Shchelkunov SN, Safronov PF, Totmenin AV, Petrov NA, Ryazankina OI, Gutorov VV, Kotwal GJ. 1998. The genomic sequence analysis of the left and right species-specific terminal region of a cowpox virus strain reveals unique sequences and a cluster of intact ORFs for immunomodulatory and host range proteins. Virology 243:432–460. https://doi.org/10.1006/viro.1998.9039.
26. Bratke KA, McLysaght A, Rothenburg S. 2013. A survey of host range genes in poxvirus genomes. Infect Genet Evol 14:406–425. https://doi.org/10.1016/j.meegid.2012.12.002.
27. Kaysser P, von Bomhard W, Dobrzykowski L, Meyer H. 2010. Genetic diversity of feline cowpox virus, Germany 2000-2008. Vet Microbiol 141:282–288. https://doi.org/10.1016/j.vetmic.2009.09.029.
28. Dabrowski PW, Radonic A, Kurth A, Nitsche A. 2013. Genome-wide comparison of cowpox viruses reveals a new clade related to variola virus. PLoS One 8:e79953. https://doi.org/10.1371/journal.pone.0079953.
29. Franke A, Pfaff F, Jenckel M, Hoffmann B, Hoper D, Antwerpen M, Meyer H, Beer M, Hoffmann D. 2017. Classification of cowpox viruses into several distinct clades and identification of a novel lineage. Viruses 9:E142. https://doi.org/10.3390/v9060142.
30. Duraffour S, Mertens B, Meyer H, van den Oord JJ, Mitera T, Matthys P, Snoeck R, Andrei G. 2013. Emergence of cowpox: study of the virulence of clinical strains and evaluation of antivirals. PLoS One 8:e55808. https://doi.org/10.1371/journal.pone.0055808.
31. Hoffmann D, Franke A, Jenckel M, Tamošiūnaitė A, Schluckebier J, Granzow H, Hoffmann B, Fischer S, Ulrich RG, Höper D, Goller K, Osterrieder N, Beer M. 2015. Out of the reservoir: phenotypic and genotypic characterization of a novel cowpox virus isolated from a common vole. J Virol 89:10959–10969. https://doi.org/10.1128/JVI.01195-15.
32. Tamošiūnaitė A, Hoffmann D, Franke A, Schluckebier J, Tauscher K, Tischer BK, Beer M, Klopfleisch R, Osterrieder N. 2016. Histopathological and immunohistochemical studies of cowpox virus replication in a three-dimensional skin model. J Comp Pathol 155:55–61. https://doi.org/10.1016/j.jcpa.2016.05.001.
33. Davies JHT, Janes LR, Downie AW. 1938. Cowpox infection in farmworkers. Lancet 232:1534–1538. https://doi.org/10.1016/S0140-6736(00)83994-X.
34. Downie AW. 1939. The immunological relationship of the virus of spontaneous cowpox to vaccinia virus. Br J Exp Pathol 20:158–176.
35. Kalthoff D, Konig P, Meyer H, Beer M, Hoffmann B. 2011. Experimental cowpox virus infection in rats. Vet Microbiol 153:382–386. https://doi.org/10.1016/j.vetmic.2011.05.048.
36. Martinez MJ, Bray MP, Huggins JW. 2000. A mouse model of aerosol-transmitted orthopoxviral disease: morphology of experimental aerosol-transmitted orthopoxviral disease in a cowpox virus-BALB/c mouse system. Arch Pathol Lab Med 124:362–377.
37. Gubser C, Bergamaschi D, Hollinshead M, Lu X, van Kuppeveld FJ, Smith GL. 2007. A new inhibitor of apoptosis from vaccinia virus and eukaryotes. PLoS Pathog 3:e17. https://doi.org/10.1371/journal.ppat.0030017.
38. Carrara G, Parsons M, Saraiva N, Smith GL. 2017. Golgi anti-apoptotic protein: a tale of camels, calcium, channels and cancer. Open Biol 7:170045. https://doi.org/10.1098/rsob.170045.
39. Hu L, Smith TF, Goldberger G. 2009. LFG: a candidate apoptosis regulatory gene family. Apoptosis 14:1255–1265. https://doi.org/10.1007/s10495-009-0402-2.
40. Saraiva M, Alcami A. 2001. CrmE, a novel soluble tumor necrosis factor receptor encoded by poxviruses. J Virol 75:226–233. https://doi.org/10.1128/JVI.75.1.226-233.2001.
41. Goujon M, McWilliam H, Li W, Valentin F, Squizzato S, Paern J, Lopez R. 2010. A new bioinformatics analysis tools framework at EMBL-EBI. Nucleic Acids Res 38:W695–W699. https://doi.org/10.1093/nar/gkq313.
42. Reynolds SE, Earl PL, Minai M, Moore I, Moss B. 2017. A homolog of the variola virus B22 membrane protein contributes to ectromelia virus pathogenicity in the mouse footpad model. Virology 501:107–114. https://doi.org/10.1016/j.virol.2016.11.010.
43. Alzhanova D, Hammarlund E, Reed J, Meermeier E, Rawlings S, Ray CA, Edwards DM, Bimber B, Legasse A, Planer S, Sprague J, Axthelm MK, Pickup DJ, Lewinsohn DM, Gold MC, Wong SW, Sacha JB, Slifka MK, Fruh K. 2014. T cell inactivation by poxviral B22 family proteins increases viral virulence. PLoS Pathog 10:e1004123. https://doi.org/10.1371/journal.ppat.1004123.
44. McKelvey TA, Andrews SC, Miller SE, Ray CA, Pickup DJ. 2002. Identification of the orthopoxvirus p4c gene, which encodes a structural protein that directs intracellular mature virus particles into A-type inclusions. J Virol 76:11216–11225. https://doi.org/10.1128/jvi.76.22.11216-11225.2002.
45. Amegadzie BY, Sisler JR, Moss B. 1992. Frame-shift mutations within the vaccinia virus A-type inclusion protein gene. Virology 186:777–782. https://doi.org/10.1016/0042-6822(92)90046-R.
46. Chang SJ, Chang YX, Izmailyan R, Tang YL, Chang W. 2010. Vaccinia virus A25 and A26 proteins are fusion suppressors for mature virions and determine strain-specific virus entry pathways into HeLa, CHO-K1, and L cells. J Virol 84:8422–8432. https://doi.org/10.1128/JVI.00599-10.
47. Patel DD, Pickup DJ, Joklik WK. 1986. Isolation of cowpox virus A-type inclusions and characterization of their major protein component. Virology 149:174–189. https://doi.org/10.1016/0042-6822(86)90119-4.
48. Ducournau C, Ferrier-Rembert A, Ferraris O, Joffre A, Favier A-L, Flusin O, Van Cauteren D, Kecir K, Auburtin B, Védy S, Bessaud M, Peyrefitte CN. 2013. Concomitant human infections with 2 cowpox virus strains in related cases France, 2011. Emerg Infect Dis 19:1996–1999. https://doi.org/10.3201/eid1912.130256.
49. Breithaupt A, Kalthoff D, Deutskens F, Konig P, Hoffmann B, Beer M, Meyer H, Teifke JP. 2012. Clinical course and pathology in rats (Rattus norvegicus) after experimental cowpox virus infection by percutaneous and intranasal application. Vet Pathol 49:941–949. https://doi.org/10.1177/0300985812439077.
50. Damaso CR, Esposito JJ, Condit RC, Moussatche N. 2000. An emergent poxvirus from humans and cattle in Rio de Janeiro State: Cantagalo virus may derive from Brazilian smallpox vaccine. Virology 277:439–449. https://doi.org/10.1006/viro.2000.0603.
51. Goyal T, Varshney A, Bakshi SK, Barua S, Bera BC, Singh RK. 2013. Buffalo pox outbreak with atypical features: a word of caution and need for early intervention! Int J Dermatol 52:1224–1230. https://doi.org/10.1111/ijd.12120.
52. Rimoin AW, Mulembakani PM, Johnston SC, Lloyd Smith JO, Kisalu NK, Kinkela TL, Blumberg S, Thomassen HA, Pike BL, Fair JN, Wolfe ND, Shongo RL, Graham BS, Formenty P, Okitolonda E, Hensley LE, Meyer H, Wright LL, Muyembe JJ. 2010. Major increase in human monkeypox incidence 30 years after smallpox vaccination campaigns cease in the Democratic Republic of Congo. Proc Natl Acad Sci U S A 107:16262–16267. https://doi.org/10.1073/pnas.1005769107.
53. Shah S. 2013. New threat from poxviruses. Sci Am 308:66–71. https://doi.org/10.1038/scientificamerican0313-66.
54. Singh RK, Hosamani M, Balamurugan V, Bhanuprakash V, Rasool TJ, Yadav MP. 2007. Buffalopox: an emerging and re-emerging zoonosis. Anim Health Res Rev 8:105–114. https://doi.org/10.1017/S1466252307001259.
55. Reynolds SE, Moss B. 2015. Characterization of a large, proteolytically processed cowpox virus membrane glycoprotein conserved in most

chordopoxviruses. Virology 483:209–217. https://doi.org/10.1016/j.virol.2015.04.014.
56. Wurbel H. 2017. More than 3Rs: the importance of scientific validity for harm-benefit analysis of animal research. Lab Anim (NY) 46:164–166. https://doi.org/10.1038/laban.1220.
57. Wargo AR, Kurath G. 2011. In vivo fitness associated with high virulence in a vertebrate virus is a complex trait regulated by host entry, replication, and shedding. J Virol 85:3959–3967. https://doi.org/10.1128/JVI.01891-10.
58. Graham SC, Bahar MW, Abrescia NG, Smith GL, Stuart DI, Grimes JM. 2007. Structure of CrmE, a virus-encoded tumour necrosis factor receptor. J Mol Biol 372:660–671. https://doi.org/10.1016/j.jmb.2007.06.082.
59. Reading PC, Khanna A, Smith GL. 2002. Vaccinia virus CrmE encodes a soluble and cell surface tumor necrosis factor receptor that contributes to virus virulence. Virology 292:285–298. https://doi.org/10.1006/viro.2001.1236.
60. Stogios PJ, Downs GS, Jauhal JJ, Nandra SK, Prive GG. 2005. Sequence and structural analysis of BTB domain proteins. Genome Biol 6:R82. https://doi.org/10.1186/gb-2005-6-10-r82.
61. Bardwell VJ, Treisman R. 1994. The POZ domain: a conserved protein-protein interaction motif. Genes Dev 8:1664–1677. https://doi.org/10.1101/gad.8.14.1664.
62. Constantinides MG, Picard D, Savage AK, Bendelac A. 2011. A naive-like population of human CD1d-restricted T cells expressing intermediate levels of promyelocytic leukemia zinc finger. J Immunol 187:309–315. https://doi.org/10.4049/jimmunol.1100761.
63. Johnston RJ, Poholek AC, DiToro D, Yusuf I, Eto D, Barnett B, Dent AL, Craft J, Crotty S. 2009. Bcl6 and Blimp-1 are reciprocal and antagonistic regulators of T follicular helper cell differentiation. Science 325:1006–1010. https://doi.org/10.1126/science.1175870.
64. Kovalovsky D, Uche OU, Eladad S, Hobbs RM, Yi W, Alonzo E, Chua K, Eidson M, Kim H-J, Im JS, Pandolfi PP, Sant'Angelo DB. 2008. The BTB-zinc finger transcriptional regulator PLZF controls the development of invariant natural killer T cell effector functions. Nat Immunol 9:1055–1064. https://doi.org/10.1038/ni.1641.
65. Piazza F, Costoya JA, Merghoub T, Hobbs RM, Pandolfi P. 2004. Disruption of PLZP in mice leads to increased T-lymphocyte proliferation, cytokine production, and altered hematopoietic stem cell homeostasis. Mol Cell Biol 24:10456–10469. https://doi.org/10.1128/MCB.24.23.10456-10469.2004.
66. Sakurai N, Maeda M, Lee SU, Ishikawa Y, Li M, Williams JC, Wang L, Su L, Suzuki M, Saito TI, Chiba S, Casola S, Yagita H, Teruya-Feldstein J, Tsuzuki S, Bhatia R, Maeda T. 2011. The LRF transcription factor regulates mature B cell development and the germinal center response in mice. J Clin Invest 121:2583–2598. https://doi.org/10.1172/JCI45682.
67. Siggs OM, Li X, Xia Y, Beutler B. 2012. ZBTB1 is a determinant of lymphoid development. J Exp Med 209:19–27. https://doi.org/10.1084/jem.20112084.
68. Swayne DE, American Association of Avian Pathologists. 1998. A laboratory manual for the isolation and identification of avian pathogens. American Association of Avian Pathologists, Jacksonville, FL.
69. Roth SJ, Hoper D, Beer M, Feineis S, Tischer BK, Osterrieder N. 2011. Recovery of infectious virus from full-length cowpox virus (CPXV) DNA cloned as a bacterial artificial chromosome (BAC). Vet Res 42:3. https://doi.org/10.1186/1297-9716-42-3.
70. Xu Z, Zikos D, Osterrieder N, Tischer BK. 2014. Generation of a complete single-gene knockout bacterial artificial chromosome library of cowpox virus and identification of its essential genes. J Virol 88:490–502. https://doi.org/10.1128/JVI.02385-13.
71. Tischer BK, Smith GA, Osterrieder N. 2010. En passant mutagenesis: a two step markerless Red recombination system. Methods Mol Biol 634:421–430. https://doi.org/10.1007/978-1-60761-652-8_30.
72. Tischer BK, von Einem J, Kaufer B, Osterrieder N. 2006. Two-step Red-mediated recombination for versatile high-efficiency markerless DNA manipulation in Escherichia coli. Biotechniques 40:191–197. https://doi.org/10.2144/000112096.
73. Langmead B, Salzberg SL. 2012. Fast gapped-read alignment with Bowtie 2. Nat Methods 9:357–359. https://doi.org/10.1038/nmeth.1923.
74. Patro R, Duggal G, Love MI, Irizarry RA, Kingsford C. 2017. Salmon provides fast and bias-aware quantification of transcript expression. Nat Methods 14:417–419. https://doi.org/10.1038/nmeth.4197.
75. R Core Team. 2017. R: a language and environment for statistical computing. R Foundation for Statistical Computing, Vienna, Austria.
76. Kärber G. 1931. Beitrag zur kollektiven Behandlung pharmakologischer Reihenversuche. Arch Exp Pathol Pharmakol 162:480–483. https://doi.org/10.1007/BF01863914.
77. Spearman C. 1908. The method of 'right and wrong cases' ('constant stimuli') without Gauss's formulae. Br J Psychol, 1904–1920 2:227–242. https://doi.org/10.1111/j.2044-8295.1908.tb00176.x.
78. Pickett BE, Sadat EL, Zhang Y, Noronha JM, Squires RB, Hunt V, Liu M, Kumar S, Zaremba S, Gu Z, Zhou L, Larson CN, Dietrich J, Klem EB, Scheuermann RH. 2012. ViPR: an open bioinformatics database and analysis resource for virology research. Nucleic Acids Res 40:D593–D598. https://doi.org/10.1093/nar/gkr859.
79. Lefkowitz EJ, Upton C, Changayil SS, Buck C, Traktman P, Buller RM. 2005. Poxvirus Bioinformatics Resource Center: a comprehensive Poxviridae informational and analytical resource. Nucleic Acids Res 33:D311–D316. https://doi.org/10.1093/nar/gki110.
80. Hemmink JD, Morgan SB, Aramouni M, Everett H, Salguero FJ, Canini L, Porter E, Chase-Topping M, Beck K, Loughlin RM, Carr BV, Brown IH, Bailey M, Woolhouse M, Brookes SM, Charleston B, Tchilian E. 2016. Distinct immune responses and virus shedding in pigs following aerosol, intra-nasal and contact infection with pandemic swine influenza A virus, A(H1N1)09. Vet Res 47:103. https://doi.org/10.1186/s13567-016-0390-5.